In vivo multiphoton kinetic imaging of the toxic effect of carbon tetrachloride on hepatobiliary metabolism

Chih-Ju Lin
Sheng-Lin Lee
Hsuan-Shu Lee
Chen-Yuan Dong

SPIE.

In vivo multiphoton kinetic imaging of the toxic effect of carbon tetrachloride on hepatobiliary metabolism

Chih-Ju Lin,[a,†] Sheng-Lin Lee,[a,†] Hsuan-Shu Lee,[b,*] and Chen-Yuan Dong[a,c,*]
[a]National Taiwan University, Department of Physics, Taipei, Taiwan
[b]National Taiwan University Hospital, Department of Internal Medicine, Taipei, Taiwan
[c]National Taiwan University, Molecular Imaging Center, Taipei, Taiwan

Abstract. We used intravital multiphoton microscopy to study the recovery of hepatobiliary metabolism following carbon tetrachloride (CCl_4) induced hepatotoxicity in mice. The acquired images were processed by a first order kinetic model to generate rate constant resolved images of the mouse liver. We found that with progression of hepatotoxicity, the spatial gradient of hepatic function disappeared. A CCl_4-induced damage mechanism involves the compromise of membrane functions, resulting in accumulation of processed 6-carboxyfluorescein molecules. At day 14 following induction, a restoration of the mouse hepatobiliary function was found. Our approach allows the study of the response of hepatic functions to chemical agents in real time and is useful for studying pharmacokinetics of drug molecules through optical microscopic imaging. © *2018 Society of Photo-Optical Instrumentation Engineers (SPIE)* [DOI: 10.1117/1.JBO.23.9.091407]

1 Introduction

As a major metabolic organ, the liver is susceptible to toxic effects from drug molecules or environment toxins. In the United States, drug-induced hepatotoxicity is a major clinical problem and accounts for more than 50% of the cases of acute liver failure.[1] Acetaminophen and temozolomide are some of the medications contributing to hepatotoxicity.[2–5] Clinically, chronic hepatitis can lead to fibrosis and cirrhosis of the liver. To study the hepatotoxic effects of drugs or toxins, acetaminophen and carbon tetrachloride (CCl_4) are popular models.[6–8] In the case of CCl_4, detoxification involves converting of the molecule into free radicals through the oxidase pathway. Eventually, the products of carbon dioxide (CO_2), carbon monoxide (CO), and hydrogen chloride (HCl) are produced.[9,10]

Toxicology, similar to many other biomedical disciplines, relies largely on histological techniques for studying the effects of toxins on hepatic physiology. Therefore, the lack of *in vivo* imaging data prevents the understanding of the mechanism of toxin-induced hepatotoxicity and dynamics of toxin-induced effects on hepatobiliary metabolism. In this study, we aim to address these issues by performing intravital multiphoton microscopy on mouse models that have been treated with CCl_4. By imaging at different time points following CCl_4 induction and performing analysis through an image-based kinetic model, we can derive image maps of rate constants depicting spatial variations of metabolic capabilities of the mouse liver.

2 Materials and Methods

The multiphoton fluorescence microscope used in this study is a home-built laser scanning unit based on an inverted microscope (Nikon TE-2000, Tokyo, Japan). The excitation source was a titanium-sapphire laser (Tsunami, Spectra-Physics, Mountain View, California) pumped by a diode-pumped solid-state laser (Millennia X, Spectra-Physics). The 780-nm laser beam was scanned in the focal plane by an x-y mirror scanning system (Model 6220, Cambridge Technology, Cambridge, Massachusetts). An oil immersion objective ($20 \times$ /NA 0.75, Plan Fluor, Nikon, Japan) was used to focus the laser beam onto the sample. With an on-sample power of around 50 mW, second harmonic generation (SHG) and fluorescence emission can be effectively excited and collected in the epi-illuminated geometry and separated into four simultaneous detection channels by dichroic mirrors (435DCXR, 495DCXR, 555DCLP, Chroma Technology, Rockingham, Vermont) and band-pass filters (HQ390/20, HQ460/50, HQ525/50, HQ610/75, Chroma Technology). In this configuration, SHG at 390 nm can be used to locate the surface of the liver by imaging the capsule (HQ390/20). Furthermore, the blue fluorescence channel can be used to identify autofluorescent hepatic stellate cells (HQ460/50). Finally, green (HQ525/50) and red (HQ610/75) fluorescence can be used to image the distribution of 6-CF and RITC-dextran labeled sinusoids. Each acquired multiphoton image is $200 \times 200 \ \mu m^2$ in area and composed of 512×512 pixels. Following the acquisition of each image, the mouse, mounted on a specimen translation stage (Prior Scientific, United Kingdom), was translated to the next position of the liver. Sequential multiphoton images are then acquired to generate a large-area image composed of 3×3 optically

---

*Address all correspondence to: Hsuan-Shu Lee, E-mail: benlee@ntu.edu.tw; Chen-Yuan Dong, E-mail: cydong@phys.ntu.edu.tw

†These authors contributed equally to this work.

scanned images. In this manner, 600×600 μm^2 of the mouse liver can be imaged in 1 min.

Prior to the acquisition of multiphoton images, wide-field fluorescence microscopy was used to identify the hepatic acinus structure. The 514-nm output of an argon laser was used for excitation. The fluorescence emission passed through a combination of a dichroic mirror (525DCLP, Chroma Technology) and band-pass filter (HQ590/80, Chroma Technology), before being imaged by a high sensitivity EM-CCD camera (iXon DV887DCS-BV, Andor Technology, Ireland).

The mice model used in this study were 7 to 8 weeks old C57BL/6 male mice and were maintained in a temperature and humidity controlled facility ($22 \pm 1°C$, $60\% \pm 5\%$), where the lighting is controlled in a 12-h on/12-h off cycle. For direct imaging of the mouse liver, an intravital hepatic imaging chamber (IHIC), made of 6Al/4V medical grade titanium alloy and a cover glass, was installed on the mouse abdomen. For IHIC installation, anesthetic, such as Zolitle 50, was applied. For CCl_4 induction, 100 μl of CCl_4 [40% (vol/vol)] was injected into the mice twice per week. To visualize the sinusoids, rhodamine B isothicyanate (RITC)-dextran with molecular weight of 70,000 was intravenously injected into the mouse. Finally, the metabolism of 6-carboxyfluorescein diacetate (6-CFDA) into 6-carboxyfluorescein (6-CF) was used for quantifying hepatobiliary
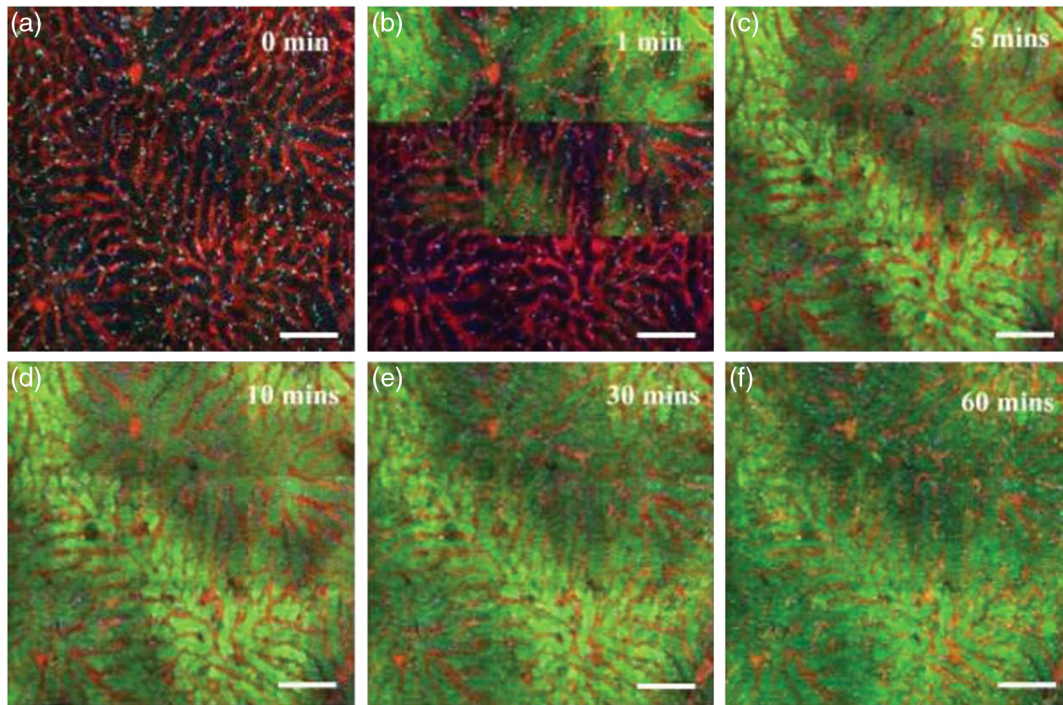

Fig. 1 Multiphoton imaging of 6-CFDA metabolism in day 1 post-CCl_4-induced hepatic injury. Time-lapse images at (a) 0 min, (b) 1 min, (c) 5 min, (d) 10 min, (e) 30 min, and (f) 60 min following 6-CFDA injection. Green: 6-CF fluorescence and red: rhodamine B-dextran labeled sinusoids. Scale bar: 100 μm.

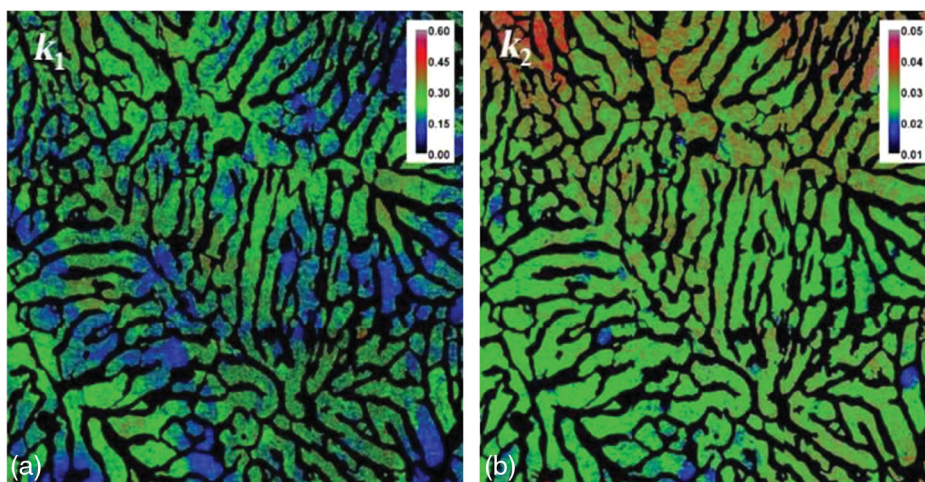**Fig. 2** (a) and (b) Kinetic rate constants (k_1 and k_2) resolve map of hepatobiliary metabolism in mouse liver (day 1 post-CCl_4 injection).
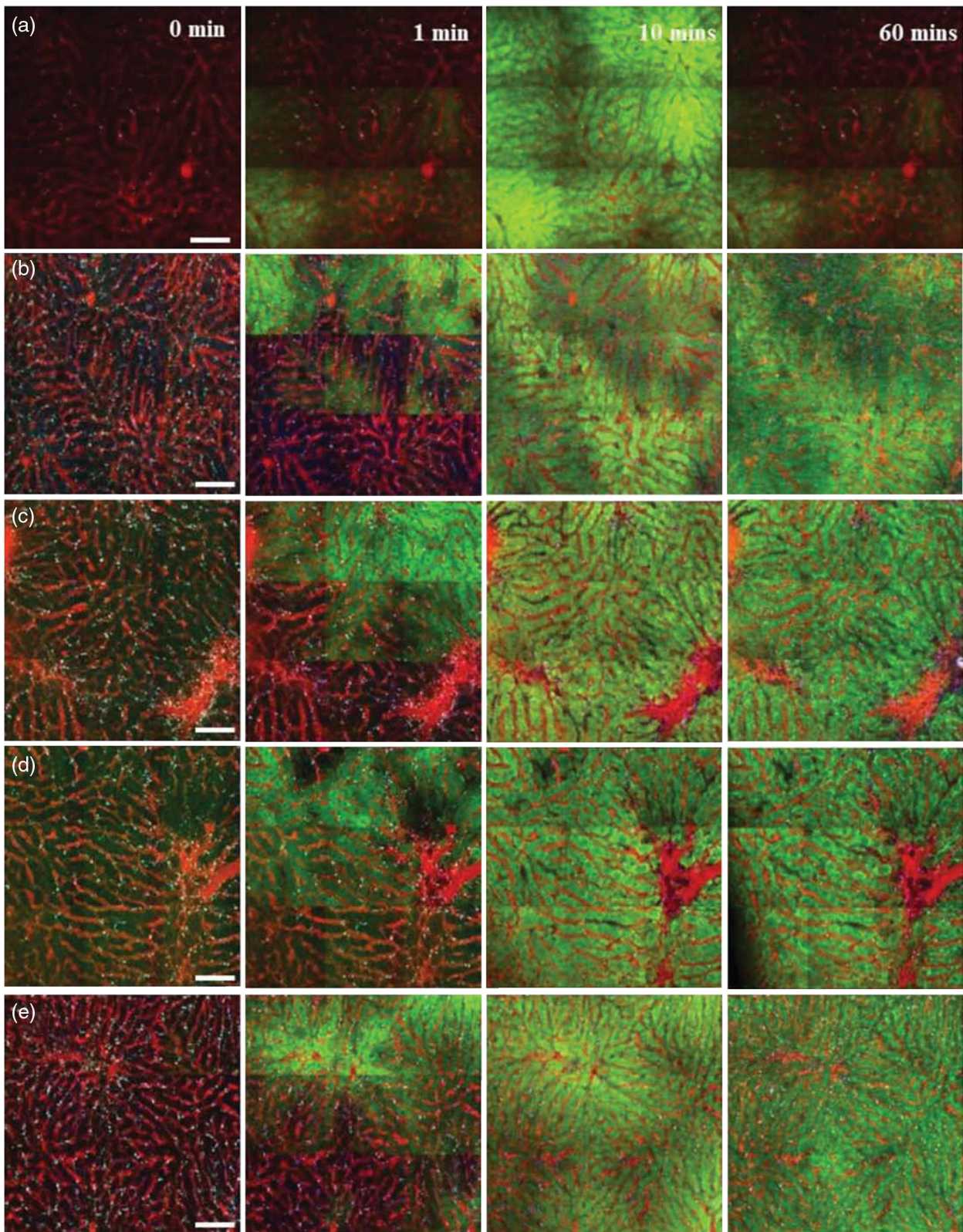
Fig. 3 *In vivo* multiphoton imaging of hepatobiliary metabolism in CCl_4-induced mice. (a) Normal, (b) day 1, (c) day 4, (d) day 7, and (e) day 14 following CCl_4 injection. Green: 6-CF fluorescence and red: rhodamine B-dextran labeled sinusoids. Scale bar: 100 μm.

metabolism. Five mice were used at each time point. The procedures for mouse treatment are similar to those described previously.[11] In order to minimize animal suffering, results of normal mice were obtained from a previous study and not repeated for this work.[12] Care and experimental protocols of the mouse model were in accordance to the regulations of the National Taiwan University Institutional Animal Care and Use Committee.

After multiphoton imaging had been performed, we used a first-order kinetic model [Eq. (1)] to fit the time-lapse images:

$$[6 - \text{CF}]_\text{H} = \frac{k_1}{k_1 - k_2}[6 - \text{CFDA}]_0 \frac{V_\text{B}}{V_\text{H}}(e^{-k_2 t} - e^{-k_1 t}). \quad (1)$$

In this model, k_1 is the rate constant used to describe uptake and intracellular esterase processing of 6-CFDA into 6-CF. k_2 is the rate constant, which accounts for the process of 6-CF

excretion into the bile canaliculi. $[6 - \text{CFDA}]_0$ is initial 6-CFDA sinusoidal concentration. $[6 - \text{CF}]_\text{H}$ is hepatocyte 6-CF concentration. V_B and V_H are the volume of the mouse blood and a hepatocyte, respectively.[12]

3 Results and Discussion

Representative time-lapse multiphoton images 1 day post-CCl$_4$-induced hepatotoxicity are shown in Fig. 1. As shown in the images, 6-CF fluorescence appeared at 1 min after 6-CFDA injection. The sinusoids are well marked by the high molecular weight RITC-dextran. Since we know the difference in time between sequentially acquired images, Eq. (1) can be used to fit for the kinetic rate constants k_1 and k_2 at each position. After processing of the time-lapse images, rate constant-resolved images can be obtained (Fig. 2). The rate constant-resolved maps show that in response to CCl$_4$ induction, different regions of the liver exhibit different metabolic response.
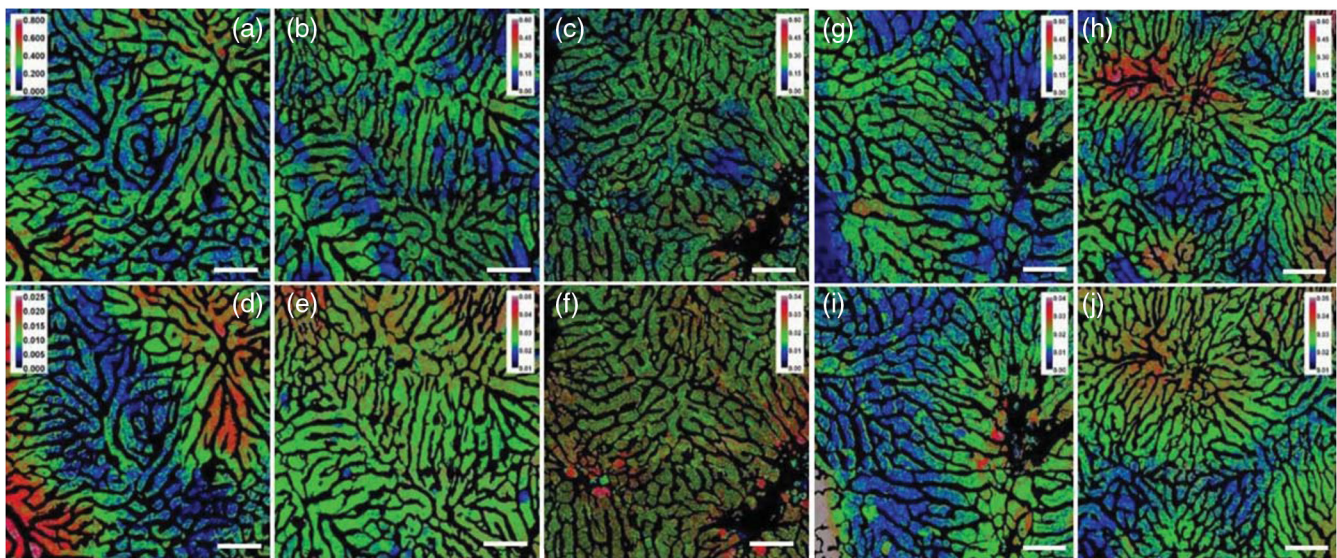

Fig. 4 Kinetic map in mice following CCl$_4$-induced hepatotoxicity. (a), (b), (c), (g), and (h) k_1-resolved images; (d), (e), (f), (i), and (j) k_2-resolved images of normal, days 1, 4, 7, and 14 post-CCl$_4$-induction mice, respectively.
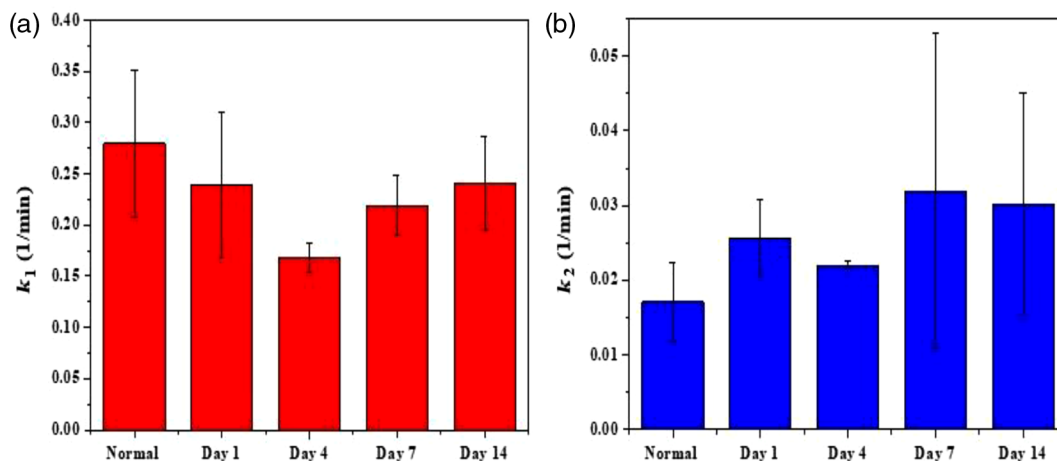

Fig. 5 Rate constants of hepatobiliary metabolism. (a) k_1 and (b) k_2 coefficients of normal, days 1, 4, 7, and 14 following CCl$_4$-induced hepatotoxicity.

In addition to the day 1 results, we also obtained time-lapse images of mice at days 4, 7, and 14 following CCl$_4$ injection. Representative time-lapse images are shown in Fig. 3.

Similarly, point-by-point analysis of the time-lapse images allows k_1 and k_2 resolved images to be derived. Representative results are shown in Fig. 4. Bar graphs of rate constants of hepatobiliary metabolism (k_1 and k_2) at normal, days 1, 4, 7, and 14 following CCl$_4$-induced hepatotoxicity are shown in Fig. 5.

The rate-constant resolved images in Fig. 4 clearly show that there is a heterogeneous distribution of hepatobiliary metabolic capabilities across the acinus. In the case of normal mouse, zone 3 of the liver acinus is most active in the uptake/processing and excretion of 6-CFDA. However, with CCl$_4$-induced hepatotoxicity, the zonal distribution of k_1 and k_2 becomes less apparent. This observation is most apparent in day 4 and is supported by the fact that the variances of the k_1 and k_2 bar graphs are the smallest for day 4 data. Interestingly, k_1 and k_2 show different trends from CCl$_4$-induced hepatotoxicity. k_1 first decreased to a minimum value at day 4 and then increased toward that of the normal mouse by day 14. On the other hand, k_2 consistently
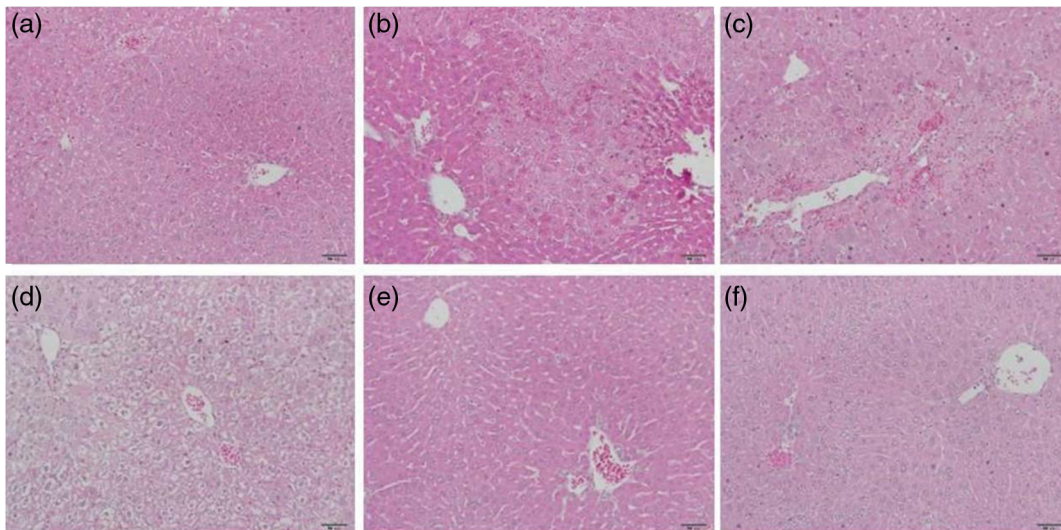

Fig. 6 Representative histological images (hematoxylin and eosin labeled) of CCl$_4$-induced liver injury. (a) Normal, (b) day 1, (c) day 2, (d) day 4, (e) day 7, and (f) day 14 following CCl$_4$ induction. Scale bar: 50 μm.
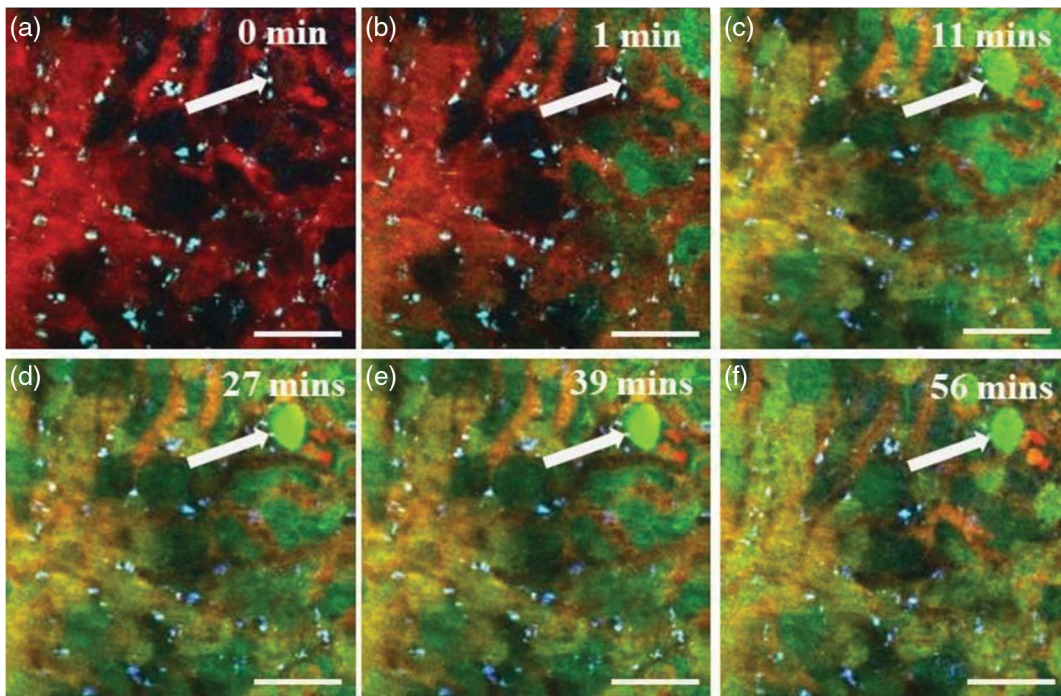

Fig. 7 Time-lapse multiphoton imaging of from CCl$_4$-induced membrane damage in hepatocytes (white arrow). Time points are (a) 0 min, (b) 1 min, (c) 11 min, (d) 27 min, (e) 39 min, and (f) 56 min. Scale bar: 50 μm.

increased once CCl_4 induction has occurred (Fig. 5). We also acquired a histological image of the mouse liver at different time points (Fig. 6). Liver damage is apparent at days 2 and 4. Near normal physiological features of the liver resume at days 7 and 14.

We also examined the possible mechanism of CCl_4-induced hepatotoxicity. As shown in the time-lapse images in Fig. 7, we would observe an increase in intracellular 6-CF fluorescence. Unlike normal hepatocytes, the intracellular 6-CF fluorescence of these hepatocytes decreases at a significantly slower rate. This observation suggests that although the uptake and processing of 6-CFDA by intracellular esterase appear normal, membrane function of the excretion of metabolites to the bile canaliculi is compromised. As a result, the processed 6-CF molecules persist in the hepatocytes. This conclusion can only be achieved through intravital microscopic examination.

4 Conclusion

In this study, we used intravital multiphoton microscopy to study the recovery of mouse liver from CCl_4-induced hepatotoxicity. In the mouse model, we found that with progression of hepatotoxicity, the zonal differences of hepatobiliary metabolism subside. Furthermore, the uptake/processing and excretion of 6-CFDA followed different kinetic pathways during the recovery process. In addition, we found that CCl_4 can hinder membrane function and hinder the excretion of the processed 6-CF molecules into the bile canaliculi. By day 14, a restoration of the mouse hepatobiliary function and physiology is complete. Although multiphoton imaging can lead to the formation of cyclobutane pyrimidine dimmers,[13,14] the lack of apparent photodamage enables our approach to be used in studying the effect of chemical agents on hepatobiliary metabolism in real time and may be applied to investigating pharmacokinetics of therapeutic drug molecules in patients under laparatomic procedures.

References

1. C. Y. Tan et al., "Mesenchymal stem cell-derived exosomes promote hepatic regeneration in drug-induced liver injury models," *Stem Cell Res. Ther.* 5, 76 (2014).
2. L. M. Grant et al., "Clinical and histological features of idiosyncratic acute liver injury caused by temozolomide," *Dig. Dis. Sci.* 58, 1415–1421 (2013).
3. N. Kaplowitz, "Idiosyncratic drug hepatotoxicity," *Nat. Rev. Drug Discovery* 4, 489–499 (2005).
4. G. Sarganas et al., "Severe sustained cholestatic hepatitis following temozolomide in a patient with glioblastoma multiforme: case study and review of data from the FDA adverse event reporting system," *Neuro-oncology* 14, 541–546 (2012).
5. P. Stock et al., "Human bone marrow mesenchymal stem cell-derived hepatocytes improve the mouse liver after acute acetaminophen intoxication by preventing progress of injury," *Int. J. Mol. Sci.* 15, 7004–7028 (2014).
6. W. Bleibel et al., "Drug-induced liver injury: review article," *Dig. Dis. Sci.* 52, 2463–2471 (2007).
7. J. V. Bruckner et al., "Oral toxicity of carbon tetrachloride: acute, subacute, and subchronic studies in rats," *Fundam. Appl. Toxicol.* 6, 16–34 (1986).
8. R. Z. Zhu et al., "Protective effect of recombinant human IL-1Ra on CCl_4-induced acute liver injury in mice," *World J. Gastroenterol.* 16, 2771–2779 (2010).
9. W. J. Brattin, E. A. Glende, Jr., and R. O. Recknagel, "Pathological mechanisms in carbon tetrachloride hepatotoxicity," *J. Free Radicals Biol. Med.* 1, 27–38 (1985).
10. L. W. Weber, M. Boll, and A. Stampfl, "Hepatotoxicity and mechanism of action of haloalkanes: carbon tetrachloride as a toxicological model," *Crit. Rev. Toxicol.* 33, 105–136 (2003).
11. H. S. Lee et al., "Optical biopsy of liver fibrosis by use of multiphoton microscopy," *Opt. Lett.* 29, 2614–2616 (2004).
12. C. J. Lin et al., "Direct visualization of functional heterogeneity in hepatobiliary metabolism using 6-CFDA as model compound," *Biomed. Opt. Express* 7, 3574–3584 (2016).
13. F. Fischer et al., "Assessing the risk of skin damage due to femtosecond laser irradiation," *J. Biophotonics* 1, 470–477 (2008).
14. O. Nadiarnykh et al., "Carcinogenic damage to deoxyribonucleic acid is induced by near-infrared laser pulses in multiphoton microscopy via combination of two- and three-photon absorption," *J. Biomed. Opt.* 17(11), 116024 (2012).

Chih-Ju Lin received his PhD in physics from National Taiwan University. His research interests are focusing on how use image to monitor and get useful information on liver metabolism. He also has excellent skills to perform animal experiments, which makes him outstanding in the related studies.

Sheng-Lin Lee earned his Dr. Sc in mechanical engineering and his master's degree in BME from Washington University in Saint Louis. He is interested in the interactions of cells and their environment. His current interests are collagen remodeling in both engineered tissue constructs and developing embryos. He is also focusing on how to utilize nonlinear microscopy as a tool to probe biological tissues.

Hsuan-Shu Lee received both his PhD and MD degrees from National Taiwan University. Currently, he is interested in the processes of emergence, proliferating, migrating, and differentiation of liver progenitor cells. He has been the owner of awards as young investigator by Academia Sinica, of medical research by the New Century Health Care Promotion Foundation, and of excellent publication by Formosan Medical Association. He has published over 60 research articles, and is a reviewer for *Hepatology, Liver International*, and *Journal of Biomedical Science*.

Chen-Yuan Dong received his PhD in the Department of Physics from the University of Urbana Champaign. He is an expert in biomedical imaging and has published studies on the application on second harmonic generation microscopy. His group focuses on developing optical techniques and the application of these techniques in elucidating fundamental biophysical processes and improving human healthcare. He is also the distinguished professor in Department of Physics in biophysics.